

Decoupled Multimodal Prototypes for Visual Recognition with Missing Modalities

Jueqing Lu
Monash University

jueqing.lu@monash.edu

Yuanyuan Qi
Monash University

yuanyuan.qi@monash.edu

Xiaohao Yang
Monash University

xiaohao.yang@monash.edu

Shujie Zhou
Monash University

shujie.zhou@monash.edu

Lan Du
Monash University

lan.du@monash.edu

Abstract

Multimodal learning enhances deep learning models by enabling them to perceive and understand information from multiple data modalities, such as visual and textual inputs. However, most existing approaches assume the availability of all modalities, an assumption that often fails in real-world applications. Recent works have introduced learnable missing-case-aware prompts to mitigate performance degradation caused by missing modalities while reducing the need for extensive model fine-tuning. Building upon the effectiveness of missing-case-aware handling for missing modalities, we propose a novel decoupled prototype-based output head, which leverages missing-case-aware class-wise prototypes tailored for each individual modality. This approach dynamically adapts to different missing modality scenarios and can be seamlessly integrated with existing prompt-based methods. Extensive experiments demonstrate that our proposed output head significantly improves performance across a wide range of missing-modality scenarios and varying missing rates.

1. Introduction

Driven by advancements in architectures like Transformers [4, 6, 11, 18, 30] and the power of pretraining on large-scale paired datasets [11, 15, 23] such as image-text pairs, multimodal learning has achieved remarkable performance across various downstream tasks, such as multimodal sentiment analysis [12]. However, most of these models assume that all data modalities are available, which limits their practicality in real-world scenarios where missing modalities are common, often due to privacy concerns, device constraints, or security limitations.

Earlier works [20, 29, 32] have attempted to mitigate the

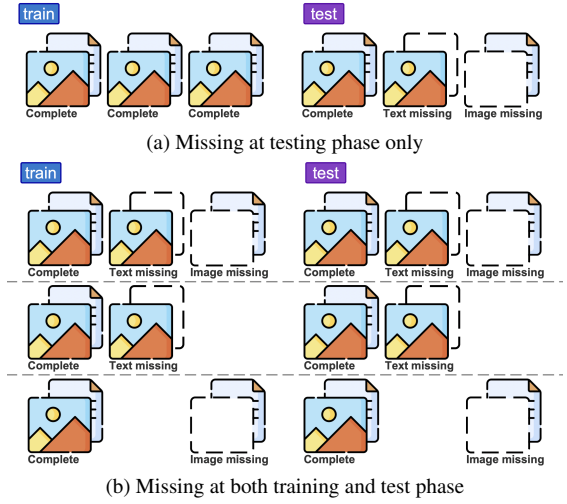


Figure 1. Demonstration of different missing modality cases.

degradation of model performance and limited applicability caused by missing modalities through reconstruction-based approaches, where missing modalities are inferred from the available ones. These methods typically assume modality completeness during training and learn an imputation function (e.g., a neural network) by simulating various missing scenarios, where instances may have different modalities missing randomly. A recent study [21] investigates the robustness of multimodal transformers by exploring different fusion methods for handling modality-incomplete data during the testing phase only (as shown in Fig. 1a). However, this approach requires fine-tuning of the entire model using complete training data. While such methods achieve promising performance when modalities are missing only during testing, their applicability remains limited in real-world scenarios when missing modalities may occur at different learning phases, including training. Therefore, in

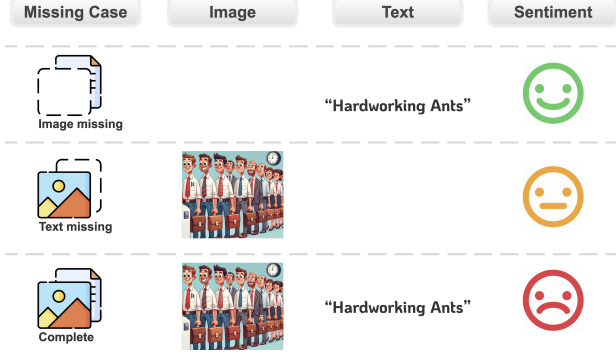


Figure 2. Multimodal sentiment example: Hardworking Ants. Missing modality can change the original sentiment.

complex scenarios of missing modalities, as illustrated in Fig. 1, the scarcity of modality-complete data can impede the effective learning of the imputation function. Additionally, Transformers are typically parameter-abundant, making fine-tuning on downstream tasks computationally expensive. This underscores more efficient adaptation methods capable of dealing with various missing scenarios across different learning phases.

Pioneering works have introduced prompt learning to handle the generalized missing modality problem, where modalities may be missing in both training and testing phases, as shown in Fig. 1b. These works also facilitate efficient fine-tuning of the Transformer model by freezing the pretrained backbone and updating only the newly introduced prompts (e.g., MAP [13] and DCP [7]). To accommodate the semantic variations induced by different missing modality scenarios (e.g., Fig. 2), some existing methods make use of missing-case-aware prompts, i.e., assigning different learnable prompts to complete inputs and various missing-modality cases. However, this case-specific adaptation is confined to the model’s encoder, overlooking the potential benefits of applying similar strategies to the output head. Nevertheless, all approaches still rely on a single shared Softmax classifier as the output head, regardless of the specific missing-modality scenarios. Inspired by the case-by-case missing-modality-aware prompt design in those methods, we extend this idea to the output head by proposing decoupled prototype learning, and argue that this could effectively improve downstream task performance. For clarity, we summarize the key differences between the missing-case-aware prompts and the decoupling we introduce at the output head in Fig. 3.

Considering the missing-case-aware decoupling, we propose Decoupled Prototype Learning (DPL) for multimodal learning to address the challenges posed by missing modalities in both training and testing. Intuitively, prototype learning assigns a data instance to a specific class based on a predefined metric (e.g., cosine similarity) between its

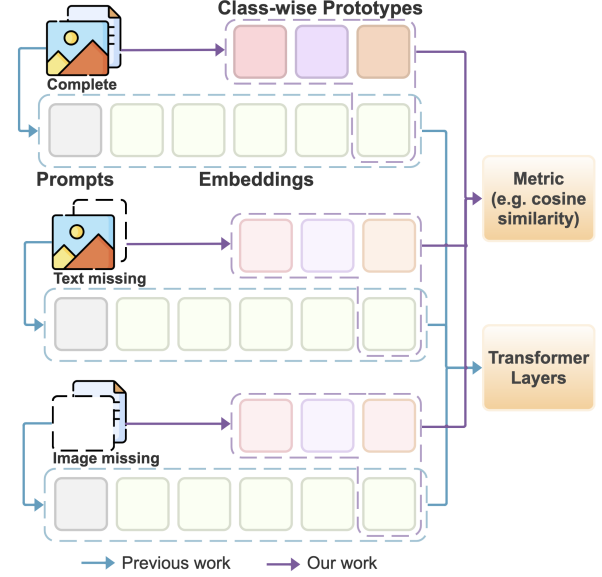


Figure 3. Missing Case-Aware Decoupling: each case is associated with its own prototypes and prompts.

representation and the class-wise prototypes. To handle different missing modality scenarios, we decouple a standard class-wise prototype into multiple modality-specific missing-case-aware prototypes. Specifically, for scenarios shown in Fig. 1b, we introduce three distinct prototypes per class: 1) a prototype for the modality-complete case, 2) a prototype for the text-missing case, and 3) a prototype for the image-missing case. Based on the modality-missing status of a given instance, the corresponding prototype is selected for metric computation, and the instance is assigned a class label accordingly. Our proposed method is orthogonal to existing prompt-based approaches for multimodal learning with missing modalities. While prompt-based methods primarily enhance the robustness of feature representations our method focuses on improving the robustness of the output head by leveraging modality missingness-aware prototypes. To evaluate the proposed DPL, we conduct experiments on three publicly available datasets: MM-IMDb, UPMC Food-101, and Hateful Memes, integrating DPL with existing methods and evaluating its performance under various scenarios.

2. Decoupled Prototype Learning (DPL)

2.1. Preliminaries

We follow prior works [7, 13] and consider the simple yet general setting for the multimodal learning with missing modalities, using an example with two modalities ($M = 2$): image (I) and text (T). For a given multimodal dataset D , its composition can include any pairwise combination of the following three sets, as well as their complete union: $\{D^C$,

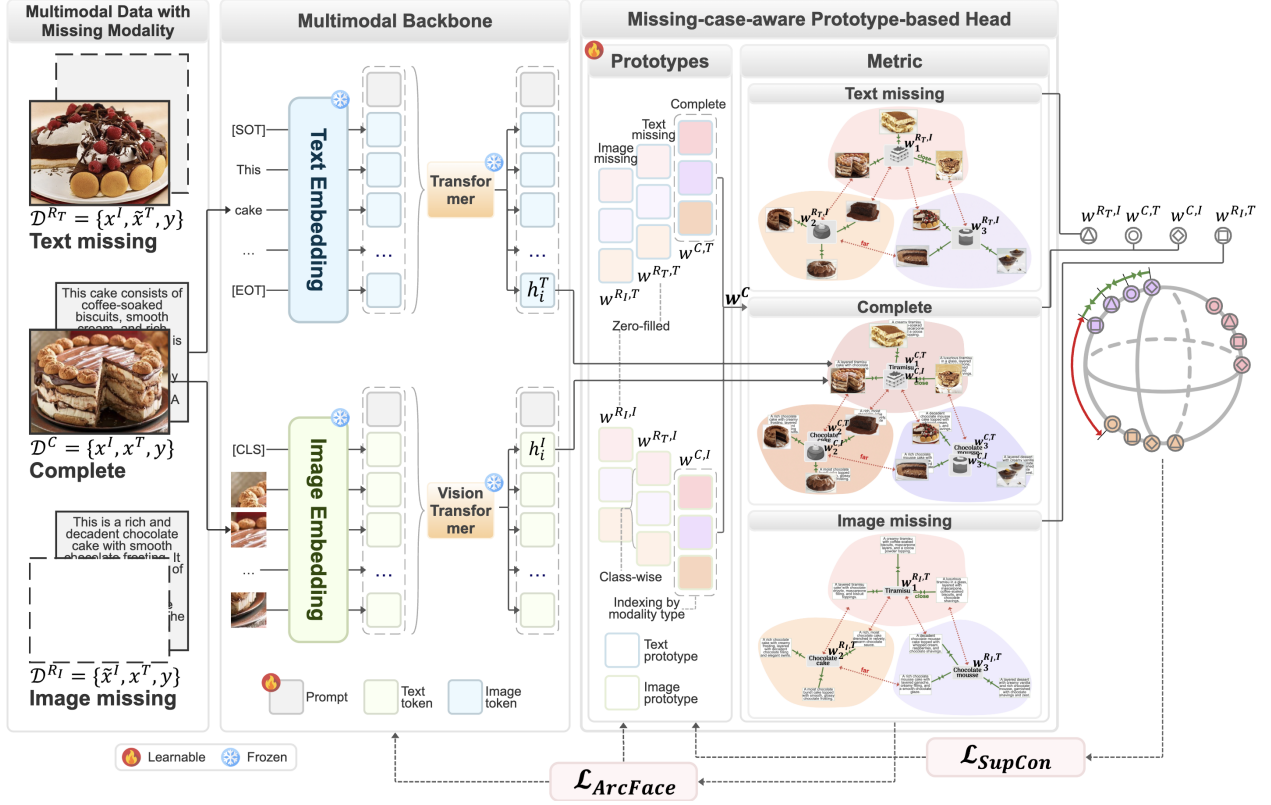


Figure 4. The framework of DPL. The modality-complete instance is shown in the flow. The indexed prototypes will be learned together with prompts via $\mathcal{L}_{ArcFace}$, and \mathcal{L}_{SupCon} is used to enhance the discriminability of those learned prototypes.

$\mathcal{D}^{R_I}, \mathcal{D}^{R_T}$ }, where \mathcal{D}^C denotes the modality-complete subset, and $\mathcal{D}^{R_I}, \mathcal{D}^{R_T}$ denote the image-missing subset and the text-missing subset, respectively. All missing cases for the $M = 2$ modalities setting are listed in Fig. 1b. For example, the last row of Fig. 1b represents a dataset, where $\mathcal{D} = \mathcal{D}^C \cup \mathcal{D}^{R_I}$.

For the multimodal recognition task, we define the these subsets as: $\mathcal{D}^C = \{x^I, x^T, y\}$, $\mathcal{D}^{R_I} = \{\tilde{x}^I, x^T, y\}$, and $\mathcal{D}^{R_T} = \{x^I, \tilde{x}^T, y\}$. Here, x^I and x^T are image and text inputs, \tilde{x}^I and \tilde{x}^T are dummy inputs (e.g., empty pixels or strings) for missing cases, and y is the class label for either multi-class or multi-label recognition.

2.2. Overall Framework

We present the overall framework in Fig. 4, which builds upon a widely used two-stream multimodal model (e.g., CLIP [23]) as the backbone. The pretrained text and image embedding layers transform the given inputs into token-level representations. Special tokens, such as [SOT] and [EOT], are added to the original text, while [CLS] serves as the special token for the image modality. Additionally, prompts are prepended not only to the original inputs but also to the hidden representations at different layers. At the final layer of each encoder, the embedding of [EOT] and

[CLS], which encapsulate the global information of text and image, are pooled for the logits computation. Prototypes are then indexed according to the missing modality case and used alongside the pooled embeddings to calculate the logits. Besides the forward pass, we also illustrate the two proposed loss terms for optimization. Learnable parameters marked by the “fire” icon in the figure will be updated via end-to-end backpropagation.

2.3. Missing-case-aware Decoupled Prototypes

We employ decoupled prototypes for multi-modal recognition in scenarios involving missing modalities. Specifically, for the k -th class in a two-modality setup (e.g., image and text), we introduce three distinct prototypes to represent each class: w_k^C , $w_k^{R_I}$ and $w_k^{R_T}$, which are tailored to those three missing cases accordingly. To further refine this approach, we decompose each of these three prototypes into modality-specific representations for each class. Since these prototypes are class-wise, they are independently defined. Consequently, the total number of prototypes is $K \times 3 \times 2$, where K is the total number of class labels, 3 accounts the three decoupled prototypes per class, and 2 represents the

number of modalities. The decomposition is formulated as:

$$w_k^C = [w_k^{C,I}, w_k^{C,T}] \quad (1)$$

$$w_k^{R_I} = [w_k^{R_I,I}, w_k^{R_I,T}] \quad (2)$$

$$w_k^{R_T} = [w_k^{R_T,I}, w_k^{R_T,T}] \quad (3)$$

For instance, $S_k^{R_T,I}$ denotes the prototype of image modality (superscript I) of the k -th class (subscript k) when text modality is missing (superscript R_T).

With regard to the multi-class recognition task, we can classify an instance $x_i \in D$ to a specific label \hat{y}_i based on $\hat{y}_i = \arg \max_k (z_i)$, where \mathbf{z}_i is a K dimensional vector that represents the logits of i -th data instance, i.e., $\mathbf{z}_i = [z_{i,1}, z_{i,2}, \dots, z_{i,k}, \dots, z_{i,K}]$. For the multi-label recognition task, we apply a sigmoid function to the logits vector, and attribute the label to the instance when the corresponding probability surpasses a predefined threshold: $\hat{y}_{i,k} = \mathbb{I}(\sigma(\mathbf{z}_{i,k}) \geq \tau)$. For example, a common threshold choice is $\tau = 0.5$, where $\sigma(\cdot)$ is a sigmoid activation function. The logits of label k , i.e., $z_{i,k}$, is calculated as follows:

$$z_{i,k} = g([h_i^I, h_i^T], w_k) \quad (4)$$

where $g(\cdot)$ is a metric function (e.g., cosine similarity) that determines how the logits are computed; h_i^I and h_i^T are the feature embeddings of the image and text modalities, respectively; w_k is the selected class-wise prototype, chosen from w_k^C , $w_k^{R_I}$ or $w_k^{R_T}$ based on the missing scenario of each individual data instance.

Specifically, for the modality-complete case ($x_i \in D^C$), the prototype in Eq. (1) is selected to compute the logits as:

$$\begin{aligned} z_{i,k} &= g([h_i^I, h_i^T], w_k^C) = g([h_i^I, h_i^T], [w_k^{C,I}, w_k^{C,T}]) \\ &= ((\hat{h}_i^I)^T \hat{w}_k^{C,I} + (\hat{h}_i^T)^T \hat{w}_k^{C,T})/2 \end{aligned} \quad (5)$$

where \hat{w}_k^{\cdot} and \hat{h}_i^{\cdot} are the L2-normalized vectors of w_k^{\cdot} and h_i^{\cdot} , ensuring that $\|\hat{w}_k^{\cdot}\|_2 = 1$ and $\|\hat{h}_i^{\cdot}\|_2 = 1$. The computed logits represent the average contribution from both modalities, a commonly used strategy in multimodal learning to unify predictions across different modalities (e.g., vision, text). Recent studies, such as prompt-based fusion [16], have demonstrated the effectiveness of averaging logits, as it not only integrates complementary information across modalities but also enhances numerical stability by maintaining balanced logits magnitudes.

For missing modality cases, we follow the most recent missing-case-aware prompt-based method DCP, which fills the hidden representation of missing modality h_i^{\cdot} with a zero padded vector $\mathbf{0}$. However, this approach causes the logits of the missing modality to become zero, making logits averaging unnecessary. To ensure compatibility with this setting, we also set the corresponding decomposed prototype to a zero padded vector. For example, in the text-missing case ($x_i \in D^{R_T}$), we assign $w_k^{R_T,T} = \mathbf{0}$, leading to the

following modified logits computation:

$$\begin{aligned} z_{i,k} &= g([h_i^I, \mathbf{0}], w_k^{R_T}) = g([h_i^I, \mathbf{0}], [w_k^{R_T,I}, \mathbf{0}]) \\ &= (\hat{h}_i^I)^T \hat{w}_k^{R_T,I} \end{aligned} \quad (6)$$

Similarly, for the image-missing instance ($x_i \in D^{R_I}$), we set $w_k^{R_I,I} = \mathbf{0}$, and the logits is computed as follows:

$$\begin{aligned} z_{i,k} &= f([\mathbf{0}, h_i^T], w_k^{R_I}) = f([\mathbf{0}, h_i^T], [w_k^{R_I,I}, w_k^{R_I,T}]) \\ &= (\hat{h}_i^T)^T \hat{w}_k^{R_I,T} \end{aligned} \quad (7)$$

2.4. Prototype Learning

We employ the Additive Angular Margin Loss (ArcFace Loss) [2] to learn the proposed decoupled prototypes, as it provides fine-grained control over the margin between different classes. The ArcFace loss is defined as:

$$\mathcal{L}_{\text{ArcFace}}^{\text{Multiclass}} = -\frac{1}{B} \sum_{i=1}^B \log \frac{e^{s(\cos(\theta_{i,y_i} + m))}}{e^{s(\cos(\theta_{i,y_i} + m))} + \sum_{k \neq y_i} e^{s \cos \theta_{i,k}}} \quad (8)$$

where s and m are two hyper-parameters that control the logits scaling and the angular margin, respectively, and $\cos \theta_{i,k}$ measures the cosine similarity between the feature embedding of data instance x_i and the prototype of the k -th class. In our approach, we set $\cos \theta_{i,k} = z_{i,k}$, because, in missing modality scenarios, (e.g., as described in Eq. 6 and Eq. 7), $z_{i,k}$ is mathematically equivalent to the cosine similarity. Additionally, in the complete modality scenario (e.g., as shown in Eq. 5), $z_{i,k}$ represents the average cosine similarity across the two modalities.

We apply the ArcFace loss with adaptive hyper-parameters in accordance with each prototypes as follows:

$$(s, m) = \begin{cases} (s^C, m^C) & \text{if } x_i \in D^C \\ (s^{R_I}, m^{R_I}) & \text{if } x_i \in D^{R_I} \\ (s^{R_T}, m^{R_T}) & \text{if } x_i \in D^{R_T} \end{cases} \quad (9)$$

The ArcFace loss is originally designed for multi-class classification task, we also modify it to accommodate the multi-label recognition task, which is updated to:

$$\mathcal{L}_{\text{ArcFace}}^{\text{Multilabel}} = -\frac{1}{B} \sum_{i=1}^B \sum_{k=1}^K (y_{i,k} \log p_{i,k} + (1 - y_{i,k}) \log(1 - p_{i,k})) \quad (10)$$

where

$$p_{i,k} = \begin{cases} \sigma(s \cos(\theta_{i,k} + m)) & \text{if } y_{i,k} = 1 \\ \sigma(s \cos \theta_{i,k}) & \text{else} \end{cases} \quad (11)$$

Meanwhile, we also explicitly model the correlation among decomposed prototypes using supervised contrastive loss. Intuitively, prototypes from same class should be close to each other, while those different classes should be well-separated. The loss is defined as follows:

$$\mathcal{L}_{\text{SupCon}} = -\sum_{k=1}^K \sum_{l=1}^K \mathbb{I}_{y_l=y_k} \mathbb{I}_{l \neq k} \log \frac{\exp(\hat{w}_k \cdot \hat{w}_l / \tau)}{\sum_{j=1}^K \mathbb{I}_{j \neq k} \exp(\hat{w}_k \cdot \hat{w}_j / \tau)} \quad (12)$$

where the τ is the scaling temperature, which is fixed to 1.0 in our experiments.

The overall training objective in DPL can be summarized to the following loss term:

$$\mathcal{L}_{DPL} = \mathcal{L}_{\text{ArcFace}} + \lambda \mathcal{L}_{\text{SupCon}} \quad (13)$$

where λ is the balancing coefficient, $\mathcal{L}_{\text{ArcFace}}$ is one of $\mathcal{L}_{\text{ArcFace}}^{\text{Multiclass}}$ and $\mathcal{L}_{\text{ArcFace}}^{\text{Multilabel}}$, selected based on the downstream task.

3. Experiments

3.1. Experiment Setup

Datasets. Following [7, 13, 21], we evaluated our DPL on three publicly accessible datasets, including

- **MM-IMdb** is a multimodal dataset designed for multilabel genre classification of movies, where each movie can be associated with multiple genres. It is one of the largest publicly available datasets for genre prediction, featuring both image and text modalities.
- **UPMC Food-101** is an extension of the ETHZ Food-101 dataset, enriched with additional text information sourced from Google Image Search. While it retains the original 101 food categories, the dataset includes some noisy image-text pairs due to its web-sourced nature.
- **Hateful Memes** is a challenging multimodal dataset developed by Facebook AI to detect hate speech in memes. The dataset is designed to prevent models from relying solely on a single modality (either text or image).

Evaluation Metrics. We adopted exactly same metrics used in [7, 13, 21] to evaluate our method. We computed the F1-Macro for evaluating multilabel recognition on the MM-IMDb dataset. For the UPMC-Food101, we used top-1 classification accuracy to evaluate the model performance. For the binary classification task on the Hateful Memes, we employed Area Under the Receiver Operating Characteristic Curve (AUROC).

Comparison Methods. Our proposed method introduces a prototype-based output head which can be seamlessly integrated with existing prompt-based methods to enhance model performance in missing modality scenarios. To evaluate its effectiveness, we select several state-of-the-art prompt-based methods: MaPLe [10], MAP, and DCP. We replaced their default output heads (e.g., Softmax or Sigmoid classification heads) with our prototype-based head, and compared performance under various missing modality conditions. Additionally, DePT [37] proposes the Channel Adjusted Transfer (CAT) head, which combines its output with the Softmax head through linear interpolation, including both logits and loss. This approach has demonstrated superior performance on modality-complete data. For a comprehensive comparison, we also included DePT as an alternative output head and report its performance.

Implementation Details. Our approach was built upon the official implementation of DCP, using CLIP as the backbone model. Specifically, ViT-B/16 was used as the visual encoder and input image was resized into 224x224. The text encoder was directly inherited from the pretrained CLIP, with the maximum text length of 77 tokens. All parameters of the pretrained encoders were frozen, except the learnable prompts and our proposed DPL. The prompt length was set to 36 for the first 6 layers of each encoder. We applied same settings to other compared methods, e.g., MaPLe and MAP. For optimization, we followed [7, 13] and used Adam optimizer with an initial learning rate of 1e-2 and a weight decay of 2e-2. The learning rate was warmed up for the first 10% of training steps and then decayed linearly to zero. Consistent with DCP, we also used a batch size of 4 on a single RTX-3090 GPU. Besides, missing modality inputs were replaced with zero-filled tensor.

Setting of Missing Modality. Following earlier works [7, 13], we simulated the missing modalities in both the training and testing phases, and used the missing rate η to control the proportion of incomplete modality data. Specifically, in the image-missing scenario ($D = D^C \cup D^{R_I}$), η indicates that $\eta\%$ of the dataset consists of text-only instances, while the remaining $1 - \eta\%$ consists of modality-complete data. Similarly, in the text-missing scenario ($D = D^C \cup D^{R_T}$), η represents the proportion of image-only instances, with the remaining $1 - \eta\%$ being modality-complete data. For the both-modalities-missing scenario ($D = D^C \cup D^{R_I} \cup D^{R_T}$), the dataset contains $\frac{\eta}{2}\%$ text-only instances, $\frac{\eta}{2}\%$ image-only instances, and $1 - \eta\%$ complete data. To evaluate the robustness of DPL, we varied the missing rate across different values (50%, 70% and 90%).

3.2. Main Results

Effectiveness. We summarized the results in Tab. 1. Our proposed DPL consistently outperforms both the default heads (e.g., Softmax or Sigmoid classifiers) and DePT’s head when integrated with different baselines, demonstrating its effectiveness in enhancing model robustness across various missing modality scenarios. Below, we provide detailed observations and discussions.

- For each prompt-based method, the proposed DPL consistently enhances model performance compared to both the default head and DePT head, showcasing its broad adaptability and consistent improvement across different approaches. For instance, on the MM-IMDb dataset, when 70% of instances are missing either text or image modality, DCP achieves absolute improvements of 4.02% and 4.07% in F1-Macro by replacing the default head and DePT head with DPL, respectively.
- Unlike DePT, which exhibits unstable performance and even performance degradation when the dataset or missing rate varies, DPL consistently outperforms both the de-

Datasets	Missing rate η	Train/Test		MaPLe (CVPR'23)			MAP (CVPR'23)			DCP (NeurIPS'24)		
		Image	Text	Default Head	DePT (CVPR'24)	DPL (ours)	Default Head	DePT (CVPR'24)	DPL (ours)	Default Head	DePT (CVPR'24)	DPL (ours)
MM-IMDb (F1-Macro)	50%	100%	50%	54.31	52.42	56.36	53.32	52.20	56.03	53.62	51.88	56.94
		50%	100%	56.90	53.28	59.01	56.97	53.87	58.91	56.50	52.86	58.70
		75%	75%	54.47	52.70	57.00	54.55	51.25	57.00	55.21	52.42	57.24
	70%	100%	30%	50.87	49.92	54.50	50.90	50.27	53.43	51.35	51.16	54.07
		30%	100%	55.99	55.02	58.56	55.10	53.78	58.17	55.87	54.58	57.69
		65%	65%	51.66	50.34	55.44	51.75	49.83	54.85	51.46	51.39	55.48
	90%	100%	10%	49.17	49.77	52.85	49.20	49.57	52.55	49.69	50.38	53.06
		10%	100%	54.57	54.17	57.50	54.66	49.83	58.02	55.07	53.73	57.35
		55%	55%	51.11	51.48	54.66	49.98	51.75	53.90	51.00	51.94	54.73
UPMC Food-101 (Accuracy)	50%	100%	50%	82.45	82.14	85.08	82.10	82.15	85.37	82.18	82.37	85.14
		50%	100%	89.18	87.31	89.92	89.15	87.05	89.89	89.36	87.35	89.83
		75%	75%	84.94	84.43	87.31	85.13	84.02	87.08	85.20	84.69	87.15
	70%	100%	30%	79.58	79.75	82.21	79.66	79.63	82.08	79.53	79.39	81.88
		30%	100%	87.80	85.93	88.11	87.51	86.27	88.23	87.56	85.83	88.06
		65%	65%	82.16	82.25	84.25	82.29	82.07	84.43	82.13	82.16	84.24
	90%	100%	10%	76.51	77.13	79.05	77.21	76.98	78.93	76.37	76.97	78.90
		10%	100%	86.23	85.17	86.39	86.39	85.30	86.49	86.26	85.06	86.68
		55%	55%	79.60	80.19	81.81	79.54	79.97	81.98	79.16	79.50	81.75
Hateful-Memes (AUROC)	50%	100%	50%	69.74	66.72	70.90	66.72	64.68	69.93	69.84	70.08	70.87
		50%	100%	64.83	65.79	66.87	63.89	61.94	64.53	65.51	64.59	66.18
		75%	75%	67.37	62.28	68.71	67.16	63.97	68.08	66.85	68.58	69.18
	70%	100%	30%	69.42	68.70	70.27	68.76	69.78	70.35	69.45	68.39	70.24
		30%	100%	63.02	63.71	64.42	60.87	62.60	63.69	62.62	62.91	65.51
		65%	65%	65.59	66.38	66.87	64.99	64.12	66.83	64.96	65.91	67.57
	90%	100%	10%	68.84	68.85	70.42	67.57	68.97	69.85	68.19	68.98	70.65
		10%	100%	60.78	61.45	61.87	62.88	61.94	63.02	62.46	60.72	62.74
		55%	55%	62.94	63.73	65.00	62.07	64.26	64.96	64.28	64.48	65.45

Table 1. Test results among different output heads with different prompt learning methods. Default head means Sigmoid head for MM-IMDb and Softmax head for UPMC Food-101 and Hateful-Memes. The best results are highlighted in **bold**.

fault head and DePT across all evaluation metrics.

- DPL further unleashes the potential of learned embeddings. For a prompt-based method with a default output head that underperforms, replacing the default head with DPL leads to significant improvements in test performance. Notably, the enhanced method can surpass the performance of other prompt-based method that originally achieved the best results with its default output head. For example, on the UPMC Food-101 dataset with 50% missing text modality, MAP performs the worst with its default Softmax output head (82.10) compared to the best-performing method, MaPLe (82.45). However, when both methods are enhanced with the DPL head, MAP surpasses MaPLe, achieving 85.37 versus 85.08.
- It is worth noting that for most datasets, such as MM-IMDb and UPMC Food-101, text inputs have a greater impact on performance. We argue that this is because text provides more detailed semantic information in textual descriptions. On the other hand, for the Hateful Memes dataset, images play a more critical role, as missing images influences the results. This difference highlights the potential impact of different fusion methods on downstream performance, which aligns with findings from previous studies [7, 21].

Efficiency. We also evaluate the efficiency of the proposed method, as illustrated in Fig. 5, using MM-IMDb as an ex-

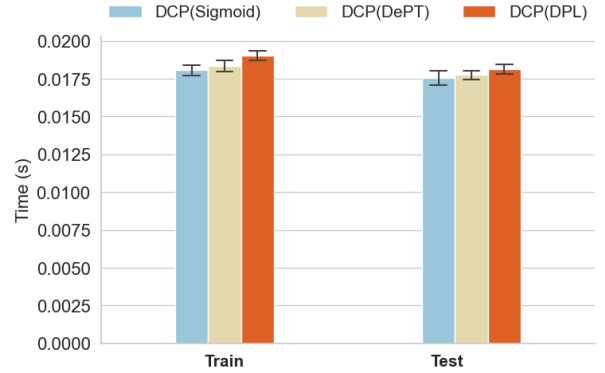


Figure 5. Efficiency comparison among different output heads. Time is measured by seconds of batch step on MM-IMDb.

ample dataset. The training time and testing time were calculated for each batch step, and the mean value is reported as the y-axis value in the bar chart. Error bars, displayed on top of each bar, represent the standard deviation of the running time across different iterations. All values were computed based on 10 independent runs to ensure statistical reliability. The training time and testing time of DPL does not increase significantly. We attribute the slight time increasing to the prototypes selection and L_{SupCon} computation.

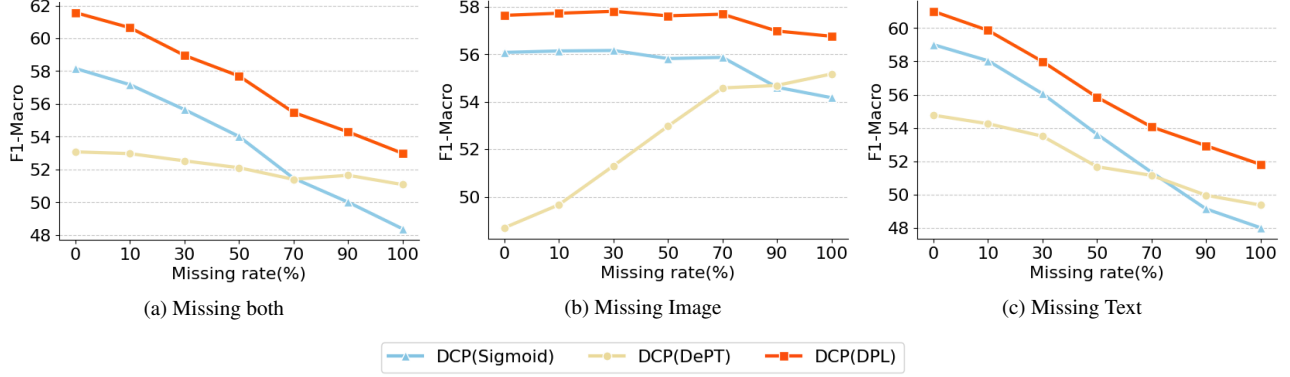


Figure 6. Testing results of various missing rates on MM-IMDb.

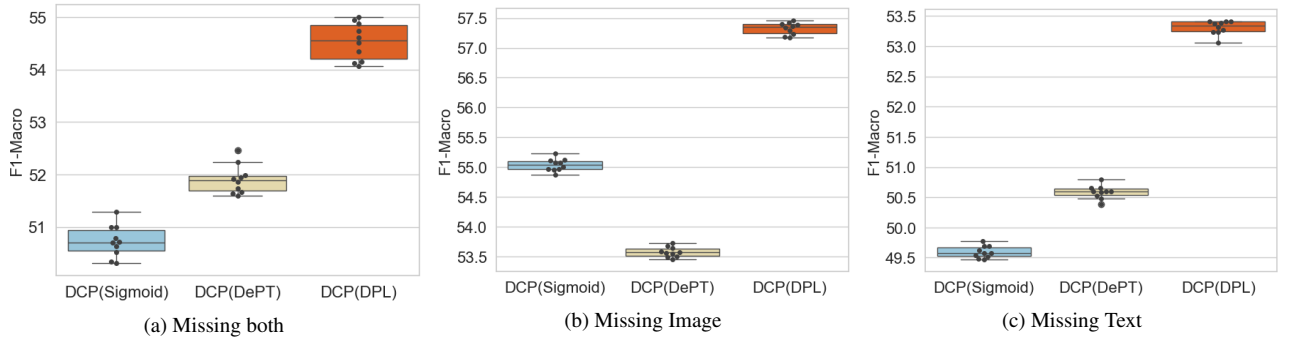


Figure 7. Testing results of varied missing modality simulations on MM-IMDb.

3.3. Robustness Analysis

Different Missing Rates. We also conducted experiments to evaluate the robustness of the proposed DPL when trained on a dataset with predefined missing rate and tested under varying missing rates. Following previous works [7, 13], we used the MM-IMDb dataset as an example, training with a 70% missing rate and evaluating its performance across different testing missing rates. As shown in Fig. 6, when combined with DCP, our method DPL (red) consistently outperforms other heads, e.g., Sigmoid (blue) and DePT (yellow), across different missing scenarios and different testing missing rates.

Varied Simulations. We also introduced a novel robustness evaluation, an aspect not previously explored in related works. In missing modality simulation, different random seeds can result in varying missing modalities patterns (e.g., missing image, missing text) and different combinations of missing modalities. As a result, the missing patterns in the test set vary across simulations. However, previous studies typically rely on a single simulation seed, limiting the assessment of model stability across different missing patterns. To comprehensively evaluate the robustness of our method, we calculated test performance across 10 different random simulations. The results, visualized in box plots in

Fig. 7, demonstrate the effectiveness of our approach. For both image-missing and text-missing scenario, our method (DPL) exhibits high consistency, as indicated by the narrow red boxes. In the both-missing scenario, although our method shows a wider inter-quartile range (IQR), it still outperforms DePT (which exhibits outliers) and Sigmoid (which performs significantly worse than DPL). Furthermore, DPL achieves a higher upper-bound, improving the best-case performance of the base method, DCP.

3.4. Ablation Study

Loss term. We conducted a set of ablation experiments to verify the effectiveness of the loss term \mathcal{L}_{SupCon} . The testing results on MM-IMDb for DCP with different output heads, including our approach, are reported in Tab. 2, where $\mathcal{L}_{ArcFace}$ is presented in Sec. 2.4. Tab. 2 shows that \mathcal{L}_{DPL} consistently outperforms $\mathcal{L}_{ArcFace}$ across different missing scenarios. Notably, the performance improvement of $\mathcal{L}_{ArcFace}$ is most pronounced in the both-missing scenario, compared to cases where only single modality is missing. We attribute this to the fact that both-missing scenario involves more decomposed prototypes in the \mathcal{L}_{SupCon} , thus incorporating more views' information.

Prototype Decomposition. We also explored another vari-

Missing rate η	Train/Test		DCP w/ DPL	
	Image	Text	$\mathcal{L}_{ArcFace}$	\mathcal{L}_{DPL}
50%	100%	50%	56.75	56.94
	50%	100%	58.67	58.70
	75%	75%	55.90	57.24
70%	100%	30%	54.15	54.07
	30%	100%	57.63	57.69
	65%	65%	54.76	55.48
90%	100%	10%	52.62	53.06
	10%	100%	57.32	57.36
	55%	55%	54.16	54.73

Table 2. Test results with different loss terms on MM-IMDb.

Missing rate η	Train/Test		DCP w/ DPL	
	Image	Text	un-decomp.	decomp.
50%	100%	50%	52.60	56.94
	50%	100%	57.89	58.70
	75%	75%	53.03	57.24
70%	100%	30%	52.73	54.07
	30%	100%	57.31	57.69
	65%	65%	52.40	55.48
90%	100%	10%	52.55	53.06
	10%	100%	55.85	57.36
	55%	55%	53.50	54.73

Table 3. Test results with different prototypes on MM-IMDb.

ation of the missing-case-aware prototypes, which are not decomposed into modality-specific ones. To assess its impact, we conducted experiments on MM-IMDb using the DCP with different output heads, and report the results in Tab. 3. As shown in Tab. 3, the decomposed prototype (denoted as “decomp.”) achieves better performance compared with un-decomposed prototypes (denoted as “un-decomp.”), which demonstrates that explicitly modeling modality-wise prototypes is crucial for improving model performance in missing modality scenarios.

4. Related Work

Multimodal Learning with Missing Modalities. The performance degradation of multimodal models due to missing modalities [21] has garnered increasing attention, as it raises critical concerns about the robustness of multimodal models. Various approaches have been proposed to enhance model’s resilience in the presence of missing modalities. For instance, MMIN [38] mitigates missing modalities by predicting intermediate features through a shared multimodal representation learned from available modalities. SMIL [20] employs a Bayesian meta-learning framework to estimate latent features for modality-incomplete data, even under extreme conditions, such as a 90% missing ratio. Ma et al. [21] investigated the robustness of multimodal transformers to missing modalities and proposed a multitask optimization framework to improve per-

formance through modality fusion. ShaSpec [32] introduces a shared head across tasks to aggregate information from diverse input samples, effectively compensating for missing modalities. Recently, MAP [13] introduces missing-aware prompts to handle missing modalities with minimal computational overhead, DCP [7] further extends MAP by explicitly modeling the correlations among prompts and their inter-relationships with input features.

Prompt Learning. Prompt learning, originally developed in NLP, uses “prompts” to guide pretrained models for downstream tasks. Early methods rely on manual prompts to improve model generalizability, while later approaches introduce learnable prompts that are optimized during training. Recently, prompt learning has been extended to multimodal tasks. CoCoOp [39] extends CoOp’s [40] soft prompts with image-conditional prompts, KgCoOp [36] aligns text embeddings with CLIP [23], MaPL [10] integrates deep prompts into both image and text branches, and DePT [37] isolates base-specific knowledge during tuning. These methods show the effectiveness of prompt learning in adapting vision-language models with minimal fine-tuning cost. Building on this, MAP and DCP integrate prompt learning into multimodal models, improving their robustness in missing-modality scenarios.

Prototype Learning. Exemplar prototypes serve as references for model predictions and inferences, playing a core role in prototype learning. This approach has demonstrated effectiveness in few-shot learning [5, 14, 26], zero-shot learning [9, 34], and has been successfully applied to face recognition [2, 3, 8, 17, 31]. Various loss functions have also been developed to improve prototype learning [2, 25, 27, 28]. Recently, conventional class-wise prototypes [35] have been extended to token-level prototypes for interpretable models [1, 19, 22, 24] and sub-centroids for visual recognition [33], leading to improved performance. Our proposed DPL builds on the ArcFace Loss, explicitly dealing with missing modality cases and capturing the correlations among prototypes. This enhances the discriminability of learned prototypes and significantly improves the model’s robustness to missing modalities, where a single shared classification head may not be sufficient.

5. Conclusion

In this work, we tackled the critical challenge of enhancing the robustness of multimodal Transformers in real-world scenarios where modalities are randomly missing. To this end, we have proposed a novel decoupled prototype-based output head, which significantly enhances the performance of existing prompt-based methods. To facilitate the effective learning of prototypes, we decomposed missing-case-aware prototypes into modality-specific components and introduced two complementary loss functions: the ArcFace loss and the supervised contrastive loss. The ArcFace loss provides fine-grained

control over the classification margin, while the supervised contrastive loss captures and models the correlations among prototypes, further enhancing their discriminability. Extensive experiments demonstrate that our proposed prototype-based output head exhibits high robustness across diverse missing modality scenarios and datasets. Moreover, it can be seamlessly integrated with existing prompt-based methods, offering a promising new direction for enhancing model robustness in missing modalities settings.

References

- [1] Chaofan Chen, Oscar Li, Daniel Tao, Alina Barnett, Cynthia Rudin, and Jonathan K Su. This looks like that: deep learning for interpretable image recognition. *Advances in neural information processing systems*, 32, 2019. 8
- [2] Jiankang Deng, Jia Guo, Niannan Xue, and Stefanos Zafeiriou. Arcface: Additive angular margin loss for deep face recognition. In *Proceedings of the IEEE/CVF conference on computer vision and pattern recognition*, pages 4690–4699, 2019. 4, 8
- [3] Jiankang Deng, Jia Guo, Jing Yang, Alexandros Lattas, and Stefanos Zafeiriou. Variational prototype learning for deep face recognition. In *Proceedings of the IEEE/CVF Conference on Computer Vision and Pattern Recognition*, pages 11906–11915, 2021. 8
- [4] Jacob Devlin. Bert: Pre-training of deep bidirectional transformers for language understanding. *arXiv preprint arXiv:1810.04805*, 2018. 1
- [5] Nanqing Dong and Eric P Xing. Few-shot semantic segmentation with prototype learning. In *BMVC*, page 4, 2018. 8
- [6] Alexey Dosovitskiy. An image is worth 16x16 words: Transformers for image recognition at scale. *arXiv preprint arXiv:2010.11929*, 2020. 1
- [7] Lianyu Hu, Tongkai Shi, Wei Feng, Fanhua Shang, and Liang Wan. Deep correlated prompting for visual recognition with missing modalities. In *Thirty-Eighth Annual Conference on Neural Information Processing Systems*, 2024. 2, 5, 6, 7, 8
- [8] Yuge Huang, Yuhan Wang, Ying Tai, Xiaoming Liu, Pengcheng Shen, Shaoxin Li, Jilin Li, and Feiyue Huang. Curricularface: adaptive curriculum learning loss for deep face recognition. In *proceedings of the IEEE/CVF conference on computer vision and pattern recognition*, pages 5901–5910, 2020. 8
- [9] Saumya Jetley, Bernardino Romera-Paredes, Sadeep Jayasumana, and Philip Torr. Prototypical priors: From improving classification to zero-shot learning. *arXiv preprint arXiv:1512.01192*, 2015. 8
- [10] Muhammad Uzair Khattak, Hanoona Rasheed, Muhammad Maaz, Salman Khan, and Fahad Shahbaz Khan. Maple: Multi-modal prompt learning. In *Proceedings of the IEEE/CVF conference on computer vision and pattern recognition*, pages 19113–19122, 2023. 5, 8
- [11] Wonjae Kim, Bokyung Son, and Ildoo Kim. Vilt: Vision-and-language transformer without convolution or region supervision. In *International conference on machine learning*, pages 5583–5594. PMLR, 2021. 1
- [12] Songning Lai, Xifeng Hu, Haoxuan Xu, Zhaoxia Ren, and Zhi Liu. Multimodal sentiment analysis: A survey. *Displays*, 80:102563, 2023. 1
- [13] Yi-Lun Lee, Yi-Hsuan Tsai, Wei-Chen Chiu, and Chen-Yu Lee. Multimodal prompting with missing modalities for visual recognition. In *IEEE Conference on Computer Vision and Pattern Recognition (CVPR)*, 2023. 2, 5, 7, 8
- [14] Gen Li, Varun Jampani, Laura Sevilla-Lara, Deqing Sun, Jonghyun Kim, and Joongkyu Kim. Adaptive prototype learning and allocation for few-shot segmentation. In *Proceedings of the IEEE/CVF conference on computer vision and pattern recognition*, pages 8334–8343, 2021. 8
- [15] Junnan Li, Dongxu Li, Caiming Xiong, and Steven Hoi. Blip: Bootstrapping language-image pre-training for unified vision-language understanding and generation. In *International conference on machine learning*, pages 12888–12900. PMLR, 2022. 1
- [16] Yaowei Li, Ruijie Quan, Linchao Zhu, and Yi Yang. Efficient multimodal fusion via interactive prompting. In *Proceedings of the IEEE/CVF conference on computer vision and pattern recognition*, pages 2604–2613, 2023. 4
- [17] Hao Liu, Xiangyu Zhu, Zhen Lei, and Stan Z Li. Adaptiveface: Adaptive margin and sampling for face recognition. In *Proceedings of the IEEE/CVF conference on computer vision and pattern recognition*, pages 11947–11956, 2019. 8
- [18] Ze Liu, Yutong Lin, Yue Cao, Han Hu, Yixuan Wei, Zheng Zhang, Stephen Lin, and Baining Guo. Swin transformer: Hierarchical vision transformer using shifted windows. In *Proceedings of the IEEE/CVF international conference on computer vision*, pages 10012–10022, 2021. 1
- [19] Chiyu Ma, Jon Donnelly, Wenjun Liu, Soroush Vosoughi, Cynthia Rudin, and Chaofan Chen. Interpretable image classification with adaptive prototype-based vision transformers. *Advances in Neural Information Processing Systems*, 37:41447–41493, 2025. 8
- [20] Mengmeng Ma, Jian Ren, Long Zhao, Sergey Tulyakov, Cathy Wu, and Xi Peng. Smil: Multimodal learning with severely missing modality. In *Proceedings of the AAAI Conference on Artificial Intelligence*, pages 2302–2310, 2021. 1, 8
- [21] Mengmeng Ma, Jian Ren, Long Zhao, Davide Testuggine, and Xi Peng. Are multimodal transformers robust to missing modality? In *Proceedings of the IEEE/CVF Conference on Computer Vision and Pattern Recognition*, pages 18177–18186, 2022. 1, 5, 6, 8
- [22] Meike Nauta, Ron Van Bree, and Christin Seifert. Neural prototype trees for interpretable fine-grained image recognition. In *Proceedings of the IEEE/CVF conference on computer vision and pattern recognition*, pages 14933–14943, 2021. 8
- [23] Alec Radford, Jong Wook Kim, Chris Hallacy, Aditya Ramesh, Gabriel Goh, Sandhini Agarwal, Girish Sastry, Amanda Askell, Pamela Mishkin, Jack Clark, et al. Learning transferable visual models from natural language supervision. In *International conference on machine learning*, pages 8748–8763. PMLR, 2021. 1, 3, 8

- [24] Dawid Rymarczyk, Łukasz Struski, Michał Górszczak, Koryna Lewandowska, Jacek Tabor, and Bartosz Zieliński. Interpretable image classification with differentiable prototypes assignment. In *European Conference on Computer Vision*, pages 351–368. Springer, 2022. 8
- [25] Florian Schroff, Dmitry Kalenichenko, and James Philbin. Facenet: A unified embedding for face recognition and clustering. In *Proceedings of the IEEE conference on computer vision and pattern recognition*, pages 815–823, 2015. 8
- [26] Jake Snell, Kevin Swersky, and Richard Zemel. Prototypical networks for few-shot learning. *Advances in neural information processing systems*, 30, 2017. 8
- [27] Kihyuk Sohn. Improved deep metric learning with multi-class n-pair loss objective. *Advances in neural information processing systems*, 29, 2016. 8
- [28] Yifan Sun, Changmao Cheng, Yuhan Zhang, Chi Zhang, Liang Zheng, Zhongdao Wang, and Yichen Wei. Circle loss: A unified perspective of pair similarity optimization. In *Proceedings of the IEEE/CVF conference on computer vision and pattern recognition*, pages 6398–6407, 2020. 8
- [29] Luan Tran, Xiaoming Liu, Jiayu Zhou, and Rong Jin. Missing modalities imputation via cascaded residual autoencoder. In *Proceedings of the IEEE conference on computer vision and pattern recognition*, pages 1405–1414, 2017. 1
- [30] A Vaswani. Attention is all you need. *Advances in Neural Information Processing Systems*, 2017. 1
- [31] Hao Wang, Yitong Wang, Zheng Zhou, Xing Ji, Dihong Gong, Jingchao Zhou, Zhifeng Li, and Wei Liu. Cosface: Large margin cosine loss for deep face recognition. In *Proceedings of the IEEE conference on computer vision and pattern recognition*, pages 5265–5274, 2018. 8
- [32] Hu Wang, Yuanhong Chen, Congbo Ma, Jodie Avery, Louise Hull, and Gustavo Carneiro. Multi-modal learning with missing modality via shared-specific feature modelling. In *Proceedings of the IEEE/CVF Conference on Computer Vision and Pattern Recognition*, pages 15878–15887, 2023. 1, 8
- [33] Wenguan Wang, Cheng Han, Tianfei Zhou, and Dongfang Liu. Visual recognition with deep nearest centroids. *arXiv preprint arXiv:2209.07383*, 2022. 8
- [34] Wenjia Xu, Yongqin Xian, Jiuniu Wang, Bernt Schiele, and Zeynep Akata. Attribute prototype network for zero-shot learning. *Advances in Neural Information Processing Systems*, 33:21969–21980, 2020. 8
- [35] Hong-Ming Yang, Xu-Yao Zhang, Fei Yin, and Cheng-Lin Liu. Robust classification with convolutional prototype learning. In *Proceedings of the IEEE conference on computer vision and pattern recognition*, pages 3474–3482, 2018. 8
- [36] Hantao Yao, Rui Zhang, and Changsheng Xu. Visual-language prompt tuning with knowledge-guided context optimization. In *Proceedings of the IEEE/CVF conference on computer vision and pattern recognition*, pages 6757–6767, 2023. 8
- [37] Ji Zhang, Shihan Wu, Lianli Gao, Heng Tao Shen, and Jingkuan Song. Dept: Decoupled prompt tuning. In *Proceedings of the IEEE/CVF Conference on Computer Vision and Pattern Recognition*, pages 12924–12933, 2024. 5, 8
- [38] Jinming Zhao, Ruichen Li, and Qin Jin. Missing modality imagination network for emotion recognition with uncertain missing modalities. In *Proceedings of the 59th Annual Meeting of the Association for Computational Linguistics and the 11th International Joint Conference on Natural Language Processing (Volume 1: Long Papers)*, pages 2608–2618, 2021. 8
- [39] Kaiyang Zhou, Jingkang Yang, Chen Change Loy, and Ziwei Liu. Conditional prompt learning for vision-language models. In *Proceedings of the IEEE/CVF conference on computer vision and pattern recognition*, pages 16816–16825, 2022. 8
- [40] Kaiyang Zhou, Jingkang Yang, Chen Change Loy, and Ziwei Liu. Learning to prompt for vision-language models. *International Journal of Computer Vision*, 130(9):2337–2348, 2022. 8